第 49 卷 第 4 期/2022 年 2 月/中国激光 研究论文

中国激光

激光光强波动无关的 248 nm 退偏器检测方法

张灵浩[1,2]，夏克贵[1,2*]，马兴华[1]，朱玲琳[1]，曾爱军[1,2**]，黄惠杰[1,2]，Sergey Avakaw[3]

[1]中国科学院上海光学精密机械研究所信息光学与光电技术实验室，上海 201800；

[2]中国科学院大学材料科学与光电工程中心，北京 100049；

[3]白俄罗斯共和国开放式股份公司“精密电子机械制造设计局-光学机械设备”，白俄罗斯 明斯克 220033

摘要 退偏器在深紫外光刻机照明系统中具有重要作用。尽管相关的设计、制造、性能评估已有一些报道，但是，相应的检测手段大多工作在可见光波段，目前仍缺乏直接对深紫外特定波长应用的退偏器进行性能检测的方法。本文提出了一种与激光光强波动无关的 248 nm 退偏器检测方法，使用 248.372 nm 波长的 KrF 准分子激光器作为光源，利用预起偏和偏振分光设计克服了激光光强波动造成的不利影响。误差分析表明，该方法适用于退偏器性能检测，绝对系统误差小于 0.1226%，随机误差约 0.2000%。验证实验和稳定性实验表明，测量偏振度均值与理论值高度一致，重复性水平与分析预期相当，再现性水平仅略差于重复性水平。这一方法为 248 nm 光刻机照明系统中使用的退偏器提供了一种稳定有效的离线性能检测手段。

关键词 测量；偏振检测；退偏器；深紫外；光刻；误差分析

中图分类号 O436.3；O439 **文献标志码** A **doi**：10.3788/CJL202249.0404003

1 引 言

随着半导体产业的发展，人们对光刻分辨率的要求越来越高。为了提高分辨率，高端光刻工艺所采用的曝光波长已发展到深紫外（DUV）乃至极紫外（EUV）波段，深紫外光刻的数值孔径已经发展到 0.5～1.35 水平[1-3]。与此同时，离轴照明技术、相移掩模技术、光学邻近效应修正技术和光瞳滤波技术等分辨率增强技术也逐步得到了研究和广泛应用[4-9]。然而，随着分辨率的提高，照明光束的偏振态对最终的成像对比度起到了关键作用[10-14]，最主要的原因是成像时存在多级次衍射光的干涉。不同级次 S 偏振光的振动方向一致，而 P 偏振光则不一致，从而使得这两个偏振分量在成像对比度上有很大差距。所以，各类偏振控制器件在高端光刻照明系统中必不可少。

退偏器是一类将入射偏振光转化为非偏振光的器件，其核心性能指标是出射光的偏振度（DOP）。其中，空间退偏器（更严格的表述是“伪”退偏器[15]，通常称为“退偏器”）通过产生空间上渐变的偏振序列来达到平均退偏的效果，这与光刻照明系统的大光束尺寸适配。关于空间退偏器设计、制造、性能评估的研究已经有很多报道[16-23]，但是，常见的偏振测量系统，如 Hinds Instruments 公司采用光弹调制法进行扫描偏振测量的 Exicor 系统[24]、Ilis 公司采用改进塞纳蒙特法进行成像偏振测量的 StrainMatic 系统[25]以及相关研究中涉及的偏振测量系统[26-27]，大多工作在可见光波段，目前尚缺乏直接对深紫外特定波长下应用的退偏器进行性能检测的方法，关键问题在于光源、偏振器件的性能不能满足高水平控制测量误差的需求。针对这一问题，本文提出并验证了一种 248 nm 退偏器检测方法，即：使用 248.372 nm KrF（氟化氪）准分子激光器作为光源，利用预起偏和偏振分光设计克服激光强度波动造成的不利影响；最后对该方法进行了测量误差水平分析和实验验证。验证实验的 DOP 测量值与

收稿日期：2021-06-02；**修回日期**：2021-07-07；**录用日期**：2021-07-28

基金项目：上海市自然科学基金面上项目（19ZR1464300）、上海市集成电路科技支撑专项（20501110600）、上海市政府间科技合作计划（20500711300）

通信作者：*kegui.xia@siom.ac.cn；**aijunzeng@siom.ac.cn

理论值高度一致，证明了该方法的有效性。重复实验结果与分析结果的误差水平相当，取得了非常低的标准差和变异系数，验证了该方法的稳定性。

2 原　　理

2.1 待测退偏器

如图 1 所示，本文中待测的退偏器由楔形石英晶体波片和楔形熔石英补偿板构成，楔形波片提供渐变的相位延迟，补偿板消除由楔角带来的光线偏折。使用穆勒算法[15]进行表征，该退偏器的穆勒矩阵 $\boldsymbol{M}$ 为

$$\boldsymbol{M}=\begin{bmatrix}1 & 0 & 0 & 0\\0 & 1 & 0 & 0\\0 & 0 & \cos(\delta) & \sin(\delta)\\0 & 0 & -\sin(\delta) & \cos(\delta)\end{bmatrix},\tag{1}$$

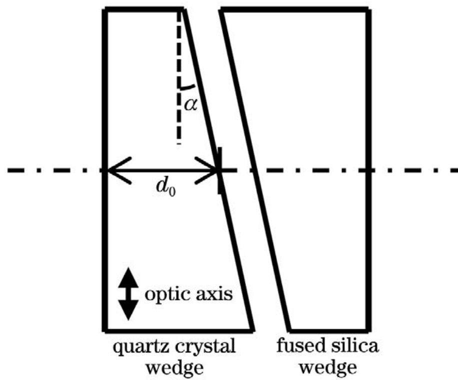

图 1　退偏器结构示意图

Fig. 1　Structure diagram of depolarizer

式中：δ 是波片的延迟量。由图 1 所示结构可知，延迟量是随空间位置变化的，其表达式为

$$\delta=\frac{\pi\Delta n D y\tan\alpha}{\lambda}+\frac{2\pi\Delta n d_0}{\lambda},\tag{2}$$

式中：Δn 为双折射率差；D 为通光孔直径；α 为楔角；λ 为波长；y 为归一化纵坐标；d_0 为波片中心的厚度。因此，退偏器的穆勒矩阵 $\boldsymbol{M}$ 在通光孔径上积分得到的平均穆勒矩阵 $\bar{\boldsymbol{M}}$ 为

$$\bar{\boldsymbol{M}}=\begin{bmatrix}1 & 0 & 0 & 0\\0 & 1 & 0 & 0\\0 & 0 & 2\cos(b)\dfrac{\mathrm{J}_1(f)}{f} & 2\sin(b)\dfrac{\mathrm{J}_1(f)}{f}\\0 & 0 & -2\sin(b)\dfrac{\mathrm{J}_1(f)}{f} & 2\cos(b)\dfrac{\mathrm{J}_1(f)}{f}\end{bmatrix},\tag{3}$$

式中：$f=\dfrac{\pi\Delta n D\tan\alpha}{\lambda}$；$b=\dfrac{2\pi\Delta n d_0}{\lambda}$；$\mathrm{J}_1$ 为一阶贝塞尔函数。当入射光为一线偏振光（即入射光的斯托克斯矢量 $\boldsymbol{S}_0=[1\quad\cos(2\theta)\quad\sin(2\theta)\quad 0]^{\mathrm{T}}$，其中 θ 为入射线偏振光的振动方向角）时，出射光束的斯托克斯矢量 $\boldsymbol{S}$ 和相应的偏振度 D_{P} 分别为

$$\boldsymbol{S}=\bar{\boldsymbol{M}}\boldsymbol{S}_0=\begin{bmatrix}1\\\cos(2\theta)\\2\cos(b)\sin(2\theta)\dfrac{\mathrm{J}_1(f)}{f}\\-2\sin(b)\sin(2\theta)\dfrac{\mathrm{J}_1(f)}{f}\end{bmatrix}=\begin{bmatrix}I\\Q\\U\\V\end{bmatrix},\tag{4}$$

$$D_{\mathrm{P}}=\frac{\sqrt{Q^2+U^2+V^2}}{I}=\sqrt{\cos^2(2\theta)+4\sin^2(2\theta)\frac{\mathrm{J}_1^2(f)}{f^2}}。\tag{5}$$

当 $\theta=45°$ 时，偏振度达到最小，$D_{\mathrm{Pmin}}=\left|\dfrac{2\mathrm{J}_1(f)}{f}\right|$。

2.2 检测方法

本文提出的 248 nm 退偏器检测方法如图 2 所示。波长为 248.372 nm 的 KrF 准分子激光器出射的光束经滤光片调整光功率后进行预起偏，预起偏后的光束经扩束后由起偏器进行起偏和分光，一路作为参考光成像于光功率计 2 上，另一路作为检测光通过退偏器样品后进行检偏并成像于光功率计 1 上。其中，退偏器样品的光轴方向为水平方向，起偏器的光轴为 45°方向，预起偏器的光轴轻微偏离 45°方向，以保证参考光可以获得足够的能量。

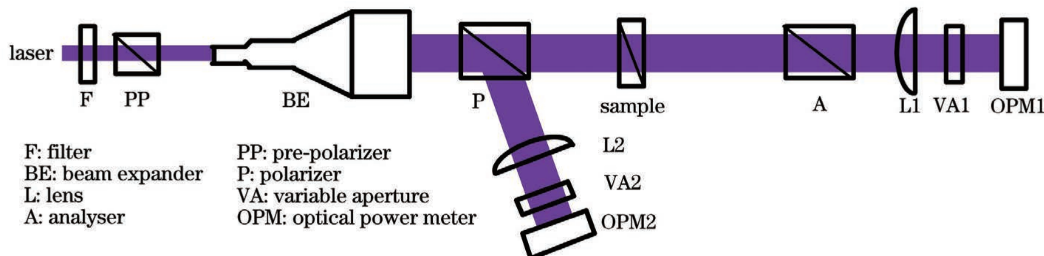

图 2　248 nm 退偏器检测方法示意图

Fig. 2　Schematic of 248 nm depolarizer detection method

该激光器的波长稳定性达到了亚纳米量级，显著减小了色散引起的测量误差，但检测中可能出现的激光光强波动会降低测量的精度和重复性，这对于退偏器这种出射 DOP 极小的器件的检测而言尤为不利。如图 3 所示，实测的 KrF 准分子激光器的出射光强波动标准差为 2.886%。但是以 DOP 等于 4%（实际上可能更小）为例，光强最大值与最小值之差仅为 8.333%，比激光器光强波动的水平（3σ=8.658%）还要小，有效信息会被随机噪声掩盖，难以得到有效的测量结果。针对这一问题，本文采用了预起偏和偏振分光设计，预起偏能消除激光器可能的出射偏振态波动对起偏器偏振分光比的影响，确保检测光与参考光的光强波动一致。分别用探测器同步记录参考光和检测光的能量数据，对检测光的能量数据进行修正，从而消除激光光强波动对测量造成的影响。光功率计前都放置可变光阑，用于调节参考光和检测光强度水平至相当量级，从而使得两台功率计具有一致的精度和灵敏度。在实际装置中，248 nm 波长下的预起偏器、起偏器和检偏器都可以用格兰激光棱镜实现，但起偏器和检偏器由于尺寸较大，消光比一般仅能确保达到数百到数千的水平，这是系统误差的重要来源。

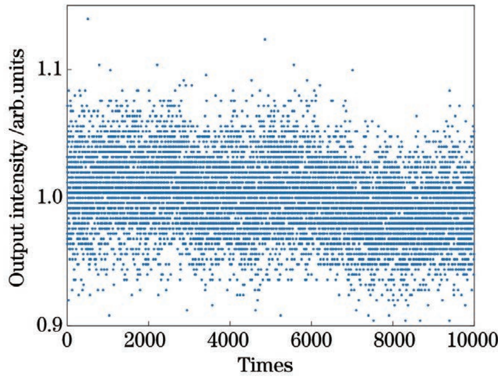

图 3 KrF 准分子激光器出射光强的 10000 次重复测量结果

Fig. 3 10000-repeated measurement results for output intensity of excimer KrF laser

装置工作时，旋转检偏器一周，同时记录参考光的光强和检偏后的光强，并进行比值处理，得到测量光强。通过拟合得到测量光强曲线，并取对应最大光强值 $I_{\max}$ 和最小光强值 $I_{\min}$，则 DOP 的测量值 D_{P} 可以表示为

$$D_{\mathrm{P}}=\frac{I_{\max}-I_{\min}}{I_{\max}+I_{\min}}\times 100\%。\tag{6}$$

3 测量误差分析

在 248.372 nm 波长下，石英晶体的双折射率差 Δn 为 0.01111，退偏器楔角 α 为 0.834°，楔形波片中心厚度为 1.374 mm，通光面直径 D 为 25 mm。以入射光振动方向与退偏器光轴的夹角（=45°）为标准角度，以第二章的原理为依据，分析本装置的测量误差水平。

入射光的振动方向偏差以及光束尺寸的变化都会带来测量误差。由（5）式模拟计算的 DOP 相对于两者的关系曲线如图 4 所示。振动方向偏差是由起偏器光轴角度偏差导致的，起偏器步进旋转精度为 0.04°，则引入的最大绝对误差为 0.1032%。光束尺寸偏差由光束发散角和退偏器光阑的尺寸精度及位置精度决定，最大偏差估计值为 0.022 mm，引入的最大绝对误差为 0.0194%。

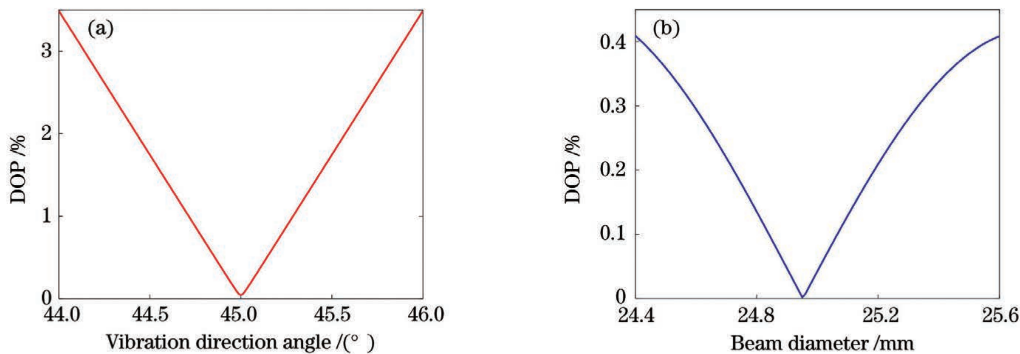

图 4 DOP 与入射光振动方向角、光束尺寸的关系曲线。(a)DOP 与入射光振动方向角的关系；(b)DOP 与光束尺寸的关系

Fig. 4 DOP versus vibration direction angle and beam size of incident light. (a) DOP versus vibration direction angle of incident light; (b) DOP versus beam diameter

起偏器和检偏器的消光比也会带来测量误差。包含有起偏器消光比 R_{PE1} 的 DOP 测量值 D_{P1} 以及包含有检偏器消光比 R_{PE2} 的 DOP 测量值 D_{P2} 的计算公式为

$$D_{\mathrm{P1}}=\frac{2I_0/(R_{\mathrm{PE1}}+1)}{I_0}=\frac{2}{R_{\mathrm{PE1}}+1},\tag{7}$$

$$D_{P2}=\frac{(I_{max0}-I_{min0})\dfrac{R_{PE2}-1}{R_{PE2}+1}}{I_{max0}+I_{min0}}=\frac{D_{P0}(R_{PE2}-1)}{R_{PE2}+1},\tag{8}$$

式中：I_{max0}、I_{min0} 和 D_{P0} 分别为无消光比误差时的检偏光强最大值、检偏光强最小值和 DOP 真实值；I_0 为入射光强。模拟计算得到的 DOP 与起偏器消光比的关系曲线如图 5(a)所示，当起偏器的消光比大于 2000∶1时，引入的最大绝对误差为 0.1000%。一般使用的退偏器要求出射 DOP 小于 5%。模拟计算得到的 DOP 测量值与真实值的绝对误差与检偏器消光比的关系曲线如图 5(b)所示，当检偏器消光比大于 500∶1 时，引入的最大绝对误差为 −0.0200%。

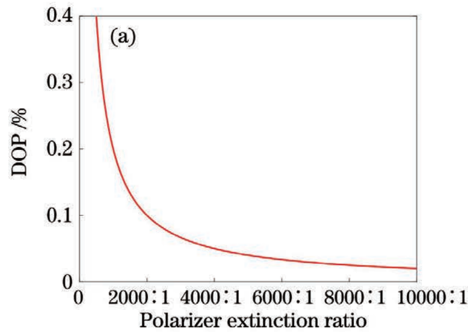

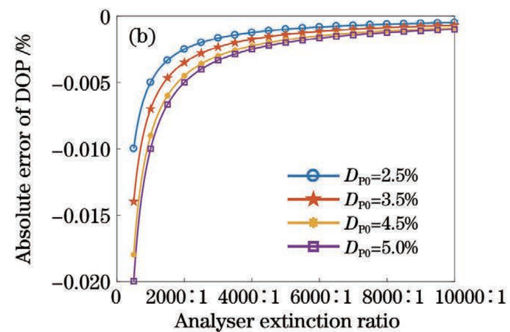

图 5 DOP 与起偏器、检偏器消光比的关系曲线。(a)DOP 与起偏器消光比的关系；(b)不同 DOP 真实值下，DOP 测量值和真实值的绝对误差与检偏器消光比的关系

Fig. 5 DOP versus extinction ratio of polarizer and analyser. (a) DOP versus polarizer extinction ratio; (b) absolute error between the measured and true DOP values versus analyser extinction ratio under different true DOP values

检偏器旋转精度和光功率计探头精度也是测量误差的来源。检偏器的旋转依赖于旋转步进电机，存在一个最小的步进角度，这会导致采集的光强最值处可能出现偏差。假设检偏器采集数据位置与实际最大、最小角度的偏差均为 β，则根据马吕斯定律可得到 DOP 测量值 D_{P3} 为

$$D_{P3}=\frac{(I_{max0}-I_{min0})(\cos^2\beta-\sin^2\beta)}{I_{max0}+I_{min0}}=D_{P0}(\cos^2\beta-\sin^2\beta)。\tag{9}$$

光功率计探头自身也存在随机误差，这会导致参考光和检测光之间光强测量值的比例关系发生轻微抖动。假设探头的随机误差为 d_p，最恶劣情形下得到的 DOP 测量值 D_{P4} 为

$$D_{P4}=\frac{(1+d_p)^2(1+D_{P0})-(1-d_p)^2(1-D_{P0})}{(1+d_p)^2(1+D_{P0})+(1-d_p)^2(1-D_{P0})}。\tag{10}$$

模拟计算得到的 DOP 测量值与真实值的绝对误差与检偏器旋转精度、光功率计探头精度的关系曲线如图 6 所示。由图 6(a)所示的绝对误差与检偏器旋转精度的关系可知，当检偏器的旋转精度小于 3°时，引入的最大绝对误差为−0.0274%。实际上经过统计学平均处理后的等效 d_p 可达到接近 0.1%的水平。由图 6(b)所示的绝对误差与真实值之间的关系可知，引入的最大绝对误差为 0.2000%。

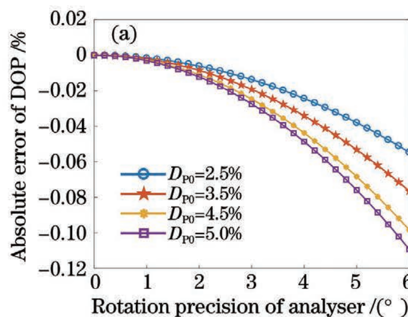

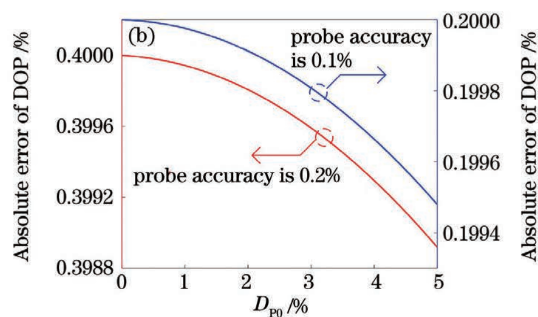

图 6 DOP 测量值和真实值的绝对误差曲线。(a)不同真实值下绝对误差与检偏器旋转精度的关系；(b)不同探头精度下绝对误差与真实值的关系

Fig. 6 Absolute error curves of measured and true DOP values. (a) Absolute error versus rotation precision of analyser under different true values; (b) absolute error versus true DOP value under different probe accuracy values

接下来对上述讨论的所有误差进行综合分析。入射光束误差和起偏器误差会导致检测时出射光的DOP真值增加，检偏器的消光比和旋转随机误差会导致DOP测量值相对于真值降低，光功率计探头精度会引起随机误差。特别地，如图5(b)、图6(a)所示，检偏误差会随着DOP真实值的增加而递增，因此本装置适用于对退偏器性能的检测，但对出射DOP较大的样品(如起偏器)将有可预见的精度下降。另外，预起偏可使起偏器消光比带来的误差大幅降低，进而可以忽略。根据一般的误差传递理论，总系统误差即为各类系统误差(含正负号)之和。但考虑到各类误差都进行了最坏估计，因此实际上单项误差的绝对值水平可能更小。不过，正误差和负误差会抵消，从而一类误差的绝对值降低反而可能会导致总系统误差增加，因此将正负误差分别累加，以绝对值更大的一个作为绝对系统误差的最坏估计。本装置预计的绝对系统误差小于0.1226%，随机误差约为0.2000%，总绝对误差约为0.3226%。

4 实验结果分析

248 nm退偏器检测实验装置如图7所示，各部件及光路如2.2节所述。为了验证所提方法的有效性和稳定性，进行了波片验证实验和退偏器性能检测。

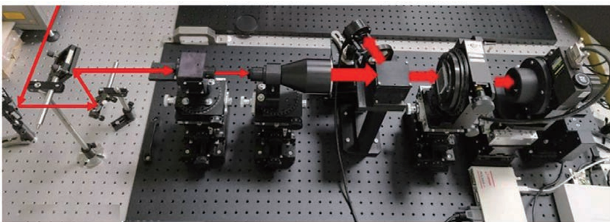

图7 248 nm退偏器检测实验装置

Fig. 7 Experimental equipment for 248 nm depolarizer detection

使用四分之一波片作为验证实验的样品。理想情况下，四分之一波片具有将入射线偏振光转换为圆偏振光的能力(快轴和入射光振动方向呈45°时)，而圆振偏光在本文检测方法下与退偏光具有相同的效果。实际的波片延迟量并不严格为四分之一波长(但可以由椭偏仪测定)，因此DOP的理论值 D_{PS} 为

$$D_{PS}=\left|\cos^2\frac{\delta}{2}-\sin^2\frac{\delta}{2}\right|。\tag{11}$$

波片的尺寸与退偏器相差甚远，但是波片转换圆偏振光的机理与通光面积无关，因此不影响测量。利用VASE椭偏仪测得的波片延迟量均值为89.285°，则DOP的理论值为1.2479%。表1展示了使用本装置对该波片进行测量的结果，DOP的均值为1.2902%，标准差为0.0458%，变异系数为3.5477%。与理论值相比，测量系统误差仅为0.0423%，证明了该方法的有效性。

表1 波片验证测试得到的DOP测量结果

Table 1 DOP measurement results obtained by wave-plate verification test

Ordinal number	DOP /%
1	1.304
2	1.333
3	1.323
4	1.300
5	1.277
6	1.237
7	1.257
8	1.367
9	1.215
10	1.289
Mean value μ /%	1.2902
Standard deviation σ /%	0.0458
Coefficient of variation C_v/%	3.5477

使用本装置对一退偏器进行了性能检测，该退偏器的结构如2.1节所述。表2展示了重复多次测

表2 退偏器DOP重复性测试结果

Table 2 DOP measurement results of depolarizer in repeatability test

Ordinal number	DOP /%
1	2.026
2	2.065
3	2.161
4	1.969
5	2.123
6	2.205
7	2.010
8	2.114
9	2.001
10	2.027
Mean value μ /%	2.0701
Standard deviation σ /%	0.0772
Coefficient of variation C_v/%	3.7287

试所得的 DOP 结果，均值为 2.0701%，标准差为 0.0772%，变异系数为 3.7287%。测量结果显示，该装置的重复性水平（$3\sigma=0.2316\%$）与分析预期（约 0.2000%）相当。为了进一步考察该装置是否能在较长时间内稳定，对该装置进行了再现性测试，即在跨越数天、样品重新放置、装置重新调试、测试人员变动等因素的叠加下，对该退偏器进行多次性能检测。表 3 展示了再现性测试所得的 DOP 结果，均值为 2.1137%，标准差为 0.1030%，变异系数为 4.8730%。再现性水平（$3\sigma=0.3090\%$）仅略差于重复性水平，表明本装置稳定性良好。

表 3 退偏器 DOP 再现性测试结果

Table 3 DOP measurement results of depolarizer in reproducibility test

Ordinal number	DOP / %
1	2.055
2	2.141
3	2.014
4	1.924
5	2.116
6	2.023
7	1.908
8	2.266
9	2.047
10	2.243
11	2.098
12	2.162
13	2.090
14	2.211
15	2.112
16	2.153
17	2.133
18	2.069
19	2.236
20	2.272
Mean value μ /%	2.1137
Standard deviation σ /%	0.1030
Coefficient of variation C_v/%	4.8730

5 结 论

为了直接对应用于深紫外特定波长下的退偏器的性能进行检测评估，选用输出波长稳定的 248.372 nm KrF 准分子激光器作为光源来设计退偏检测方法，并利用预起偏和偏振分光设计克服了激光光强波动造成的测量难题。对该方法的测量误差进行量化分析，分析结果表明，该方法适用于退偏器性能检测，绝对系统误差小于 0.1226%，随机误差约为 0.2000%，总绝对误差约为 0.3226%。

为了验证该方法的有效性和稳定性，搭建了一套实验装置，并采用该装置对四分之一波片样品和退偏器样品分别进行了检测。波片验证结果表明，DOP 测量值与理论值高度一致，测量系统误差仅为 0.0423%，证明了该方法的有效性。退偏器检测结果表明该装置的重复性水平（$3\sigma=0.2316\%$）与分析预期相当，再现性水平（$3\sigma=0.3090\%$）仅略差于重复性水平，具有良好的性能稳定性。

本工作为 248 nm 光刻机照明系统中使用的退偏器提供了一个稳定有效的离线性能检测方法，具有重要的实际意义。未来将对其进行进一步开发研究，以满足更短波长光刻系统的需求。

致谢 感谢蒲柯松工程师在开发编写装置运行程序方面提供的帮助！感谢王振工程师在机械加工方面提供的支持！

参 考 文 献

[1] Bruning J H. Optical lithography: thirty years and three orders of magnitude: the evolution of optical lithography tools[J]. Proceedings of SPIE, 1997, 3049: 14-27.

[2] Fay B. Advanced optical lithography development, from UV to EUV[J]. Microelectronic Engineering, 2002, 61/62: 11-24.

[3] Yuan Q Y, Wang X Z. Recent development of international mainstream lithographic tools[J]. Laser & Optoelectronics Progress, 2007, 44(1): 57-64.
袁琼雁, 王向朝. 国际主流光刻机研发的最新进展[J]. 激光与光电子学进展, 2007, 44(1): 57-64.

[4] Rizvi S A. National technology roadmap for semiconductors: an analysis and perspective[J]. Proceedings of SPIE, 1998, 3331: 190-196.

[5] Zhang Y Q, Wu R M, Zheng Z R. Freeform surface off-axis illumination design with the Monge-Ampère equation method in optical lithography[J]. Applied Optics, 2014, 53(31): 7296-7303.

[6] Chen M, Zhang F, Zeng A J, et al. Method of pupil shaping for off-axis illumination in optical lithography [J]. Journal of Optical Technology, 2016, 83(3):

154-158.

[7] Oh S, Han D D, Shim H B, et al. Optical proximity correction (OPC) in near-field lithography with pixel-based field sectioning time modulation[J]. Nanotechnology, 2018, 29(4): 045301.

[8] Shen Y J, Peng F, Zhang Z R. Efficient optical proximity correction based on semi-implicit additive operator splitting[J]. Optics Express, 2019, 27(2): 1520-1528.

[9] Zhu S Y, Yang B X, Ma X Z, et al. Research on high energy efficiency pupil correction based on multi-ring partition in photolithography machine[J]. Chinese Journal of Lasers, 2021, 48(17): 1704001.
朱思羽, 杨宝喜, 马晓喆, 等. 光刻机环状多分区高能量利用率光瞳校正研究[J]. 中国激光, 2021, 48(17): 1704001.

[10] Flagello D G, Mulkens J, Wagner C. Optical lithography into the millennium: sensitivity to aberrations, vibration, and polarization[J]. Proceedings of SPIE, 2000, 4000: 172-183.

[11] Totzeck M, Graupner P, Heil T, et al. How to describe polarization influence on imaging[J]. Proceedings of SPIE, 2005, 5754: 23-37.

[12] Pang W B, Cen Z F, Li X T, et al. The effect of polarization light on optical imaging system[J]. Acta Physica Sinica, 2012, 61(23): 234202.
庞武斌, 岑兆丰, 李晓彤, 等. 偏振对光学系统成像质量的影响[J]. 物理学报, 2012, 61(23): 234202.

[13] Luo H M, Cen Z F, Li X T, et al. Polarization analysis of a real high numerical aperture optical lithography[J]. Acta Optica Sinica, 2013, 33(11): 1122002.
罗红妹, 岑兆丰, 李晓彤, 等. 实际高数值孔径光刻系统的偏振分析[J]. 光学学报, 2013, 33(11): 1122002.

[14] Dejkameh A, Erdmann A, Evanschitzky P, et al. Fourier ptychography for lithography high NA systems[J]. Proceedings of SPIE, 2018, 10694: 106940B.

[15] Kliger D S, Lewis J W, Randall C E. Polarized light in optics and Spectroscopy[M]. San Diego, CA, USA: Academic Press, 1990.

[16] McClain S C, Chipman R A, Hillman L W. Aberrations of a horizontal-vertical depolarizer[J]. Applied Optics, 1992, 31(13): 2326-2331.

[17] Zhang D Y, Luo F, Luo Y Q, et al. Cholesteric liquid crystal depolarizer[J]. Optical Engineering, 2007, 46(7): 070504.

[18] Bagan V A, Davydov B L, Samartsev I E. Characteristics of Cornu depolarisers made from quartz and paratellurite optically active crystals[J]. Quantum Electronics, 2009, 39(1): 73-78.

[19] Song S X, Song L K. Analysis of double plate rotation depolarizer by Mueller matrix[J]. Acta Optica Sinica, 2009, 29(7): 1947-1950.
宋师霞, 宋连科. 双光楔旋光退偏器的 Mueller 矩阵分析[J]. 光学学报, 2009, 29(7): 1947-1950.

[20] de Sande J C, Santarsiero M, Piquero G, et al. Longitudinal polarization periodicity of unpolarized light passing through a double wedge depolarizer[J]. Optics Express, 2012, 20(25): 27348-27360.

[21] Liu X L, Li M, An N, et al. Design and analysis of dual Babinet depolarizer applied to rectangular pupils [J]. Laser & Optoelectronics Progress, 2018, 55(8): 082601.
刘晓林, 李明, 安宁, 等. 矩形光瞳下双巴比涅型消偏器的设计与分析[J]. 激光与光电子学进展, 2018, 55(8): 082601.

[22] Tian J W, Xue Q S, Lu F Q, et al. Design and analysis of depolarizer for space-borne grating-dispersion type spectrometer[J]. Acta Optica Sinica, 2019, 39(3): 0313001.
田杰文, 薛庆生, 鲁凤芹, 等. 星载光栅色散型光谱仪消偏器的设计与分析[J]. 光学学报, 2019, 39(3): 0313001.

[23] Li M X, Li H, Zhang S Q, et al. The manufacture of depolarizer in transform system of immersion photolithography polarization state[J]. Proceedings of SPIE, 2019, 11334: 113340T.

[24] Wang B L, Hellman W. Accuracy assessment of a linear birefringence measurement system using a Soleil-Babinet compensator[J]. Review of Scientific Instruments, 2001, 72(11): 4066-4070.

[25] Katte H. Imaging measurement of stress birefringence in optical materials and components[J]. Photonik International, 2009, 1: 39-41.

[26] Mao J H, Wang Y M, Shi E T, et al. Design and test of depolarizer for space-borne imaging spectrometer [J]. Acta Optica Sinica, 2017, 37(4): 0423001.
毛靖华, 王咏梅, 石恩涛, 等. 星载成像光谱仪退偏器的设计及测试[J]. 光学学报, 2017, 37(4): 0423001.

[27] Kalbarczyk A, Jaroszewicz L R, Bennis N, et al. The young interferometer as an optical system for a variable depolarizer characterization[J]. Sensors, 2019, 19(14): 3037.

Detection Method for 248 nm Depolarizer Independent of Laser Intensity Fluctuation

Zhang Linghao[1,2], Xia Kegui[1,2*], Ma Xinghua[1], Zhu Linglin[1], Zeng Aijun[1,2**], Huang Huijie[1,2], Sergey Avakaw[3]

[1] *Laboratory of Information Optics and Optoelectronic Technology, Shanghai Institute of Optics and Fine Mechanics, Chinese Academy of Sciences, Shanghai* 201800, *China*;

[2] *Center of Materials Science and Optoelectronics Engineering, University of Chinese Academy of Sciences, Beijing* 100049, *China*;

[3] *Company of KBTEM-OMO Republication Unitary Scientific and Production Enterprise, Minsk* 220033, *Belarus*

Abstract

Objective With the development of the semiconductor industry, the requirement for photolithography resolution is significantly increasing. As the resolution increases, the polarized illumination is required to improve the image contrast. Depolarizers are devices that convert incident-polarized light into unpolarized light, with the degree of polarization (DOP) of the output light as a core performance index. Depolarizer plays an essential role in the deep ultraviolet (DUV) lithography tool illumination system. Despite some reports on design, manufacture, and performance evaluation, most traditional detection methods work in the visible band. There is still no direct method for detecting the performance of the depolarizer for specific DUV wavelength applications. The key problem is that the high-level control requirement of the measurement error contradicts the insufficient performance of the light source and polarizing devices. To solve this problem, this study proposes a method for detecting 248 nm depolarizer independent of laser intensity fluctuation (Fig. 2 Schematic of the method, Fig. 7 Experimental equipment). The 248.372 nm excimer krypton fluoride (KrF) laser is used as the light source. The adverse effects caused by the laser intensity fluctuation are overcome through pre-polarizing and polarization beam splitting design. The measurement error is analyzed and verified experimentally. The DOP measurement value is highly consistent with the theoretical value, verifying the validity of the proposed method. The DOP results in the repeatability and reproducibility tests show very low standard deviations and variation coefficients, which are consistent with the analysis level. The proposed method provides a stable and effective tool for offline performance detection of the depolarizer used in the 248 nm lithography tool illumination system.

Methods To detect the depolarizer used in 248 nm lithography, the light source needs to be monochromatic and high powered to eliminate dispersion and be effective under the conditions of a large beam area and a low transmittance of each device. Only the excimer KrF laser is suitable for the requirement. However, measured standard deviation of the emitted light intensity is 2.886% (Fig. 3); thus, the 3σ of 8.658%, even larger than the theoretical difference between the maximum and minimum light intensity in DOP measurement. For example, if DOP is 4%, the theoretical difference is only 8.333%. The valid information will be covered by random noise, making it difficult to obtain effective measurement results. We use pre-polarizing and polarization beam splitting designs to overcome this difficulty. The reference light and detection light synchronously reflect the light intensity fluctuation. Therefore, the fluctuation can be eliminated by the division operation. The pre-polarizing design can eliminate the interference of the polarization fluctuation of the light source on the polarization splitting ratio. Additionally, we quantitatively analyze six types of errors (Figs. 4–6) and distinguish the target and effect of each error, including their summary. We also conduct verification experiments and stability tests. The quarter-wave plate (QWP) can convert the incident linearly-polarized light into a circularly-polarized light, which has the same effect as a depolarized light in the detection. The actual retardation of QWP is not strictly a quarter wavelength but can be measured using an ellipsometer. The theoretical value of DOP is determined by retardation. Therefore, QWP can be used as a standard sample to verify the validity of the proposed method. Furthermore, repeatability and reproducibility measurements of the depolarizer sample can verify the stability of the proposed method.

Results and Discussions The error analysis shows that the proposed method is highly suitable for performance detection of samples with small DOP, such as depolarizers. The absolute system, random, and total absolute errors

are less than 0.1226%, ~0.2000%, and ~0.3226%. In the verification experiments, the mean retardation of the QWP measured using a VASE ellipsometer is 89.285° and the theoretical value of DOP is 1.2479%. The measured DOP using this device is 1.2902%, the standard deviation is 0.0458%, and the coefficient of variation is 3.5477% (Table 1). Compared with the theoretical values, the measurement system error is only 0.0423%, confirming the validity of the proposed method. In the repeatability test, the DOP of the depolarizer is measured with a mean, standard deviation, and coefficient of variation of 2.0701%, 0.0772%, and 3.7287%, respectively (Table 2). The measurement results show that the repeatability level of the device ($3\sigma = 0.2316\%$) is consistent with the analysis expectation (~0.2000%). In the reproducibility test, the DOP of the depolarizer is measured with a mean, standard deviation, and coefficient of variation of 2.1137%, 0.1030%, and 4.8730%, respectively (Table 3). The reproducibility level ($3\sigma = 0.3090\%$) is only slightly worse than the repeatability level, indicating the stability of the device.

Conclusions This study proposes a detection method for the 248 nm depolarizer independent of laser intensity fluctuation. We selecte an excimer KrF laser with a stable output wavelength of 248.372 nm as the light source. The adverse effects caused by the light intensity fluctuation are overcome through pre-polarizing and polarization splitting design. The error analysis shows that the proposed method is suitable for performance detection of the depolarizer. The absolute system error is less than 0.1226%, and the random error is ~0.2000%. The verification experiments show that the measured mean DOP is highly consistent with the theoretical value. It also shows that the measurement system error is only 0.0423%, confirming the validity of the proposed method. The stable test shows the repeatability level ($3\sigma = 0.2316\%$) is consistent with the analysis expectation (~0.2000%), and the reproducibility level ($3\sigma = 0.3090\%$) is only slightly worse than the repeatability level, indicating the stability of the device. Therefore, the proposed method provides a stable and effective tool for offline performance detection of the depolarizer used in the 248 nm lithography tool illumination system. Furthermore, the method is essential and should be further developed to meet the requirements of shorter wavelength lithography systems.

Key words measurement; polarization detection; depolarizer; deep ultraviolet; optical lithography; error analysis